The momentum spectrum of muons at sea level in the range 5-1200 GeV/c

1972 J. Phys. A: Gen. Phys. 5 1384

(http://iopscience.iop.org/0022-3689/5/9/011)

J. Phys. A: Gen. Phys., Vol. 5, September 1972. Printed in Great Britain. © 1972.

The momentum spectrum of muons at sea level in the range 5–1200 GeV/*c*

B C NANDI and M S SINHA

Department of Physics, Regional Engineering College, Durgapur, India

MS received 9 December 1971, in final revised form 17 April 1972

Abstract. The momentum spectrum of sea level cosmic ray muons has been measured for near vertical incidence in the range $5\,\mathrm{GeV}/c < p < 1200\,\mathrm{GeV}/c$ by the Durgapur cosmic ray spectrograph. The measured spectrum compares well with that predicted from the pion diffusion model based on the assumption of 100% pions as the parent of muons. The exponent of the pion production spectrum has been determined to be $-2{\cdot}61^{+0{\cdot}03}_{-0{\cdot}02}$. The present results are compared with the results of other workers.

1. Introduction

The muon component of the cosmic radiation at sea level is the progeny of such particles as hyperons, charged pions and kaons which are produced in the interaction of the primary cosmic radiation with the air nuclei in the upper atmosphere. The nature of the interaction by which the secondary cosmic rays are produced and the effect of the geomagnetic field on the muon beam can be examined from the experimental study of the momentum spectrum of muons and its comparison with the expected spectrum.

The justification for yet another measurement of the muon spectrum is that this is an important parameter of the cosmic radiation being related, as it is, to both the characteristics of high energy interactions referred to above and a variety of measurements underground. At present, interest centres on the absolute intensity at low energy, the shape of the spectrum over the whole range and the angular variation of intensity of muons. In the present work we concentrate on the spectral shape for near vertical particles. Here, useful results may be achieved from an instrument of only modest size because most of the discrepancies which occur between the results of different workers come not from statistical errors but from bias effects of various kinds. The results are normalized to very recent absolute intensities, comparisons are made with other data and the parameters of the production spectrum of the parent pions are determined.

The measurement of the near vertical muon spectrum reported here was carried out at Durgapur, India at an altitude of 360 ft and 12 °N geomagnetic latitude by means of the Durgapur cosmic ray spectrograph.

2. The spectrograph

A schematic diagram of the spectrograph is shown in figure 1. The characteristics of the spectrograph have been described by Nandi and Sinha (1969); essentially it consists

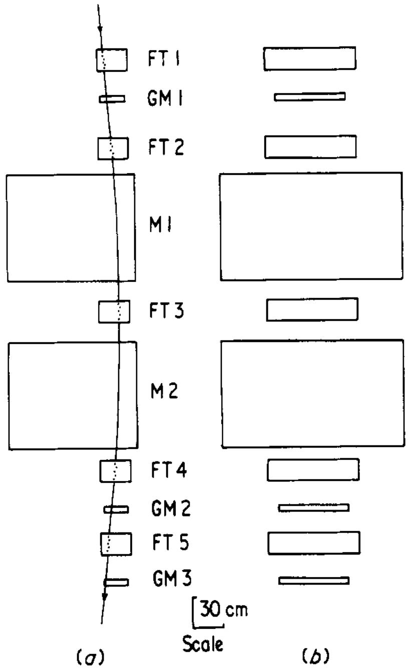

Figure 1. Schematic diagram of the Durgapur spectrograph: M1, M2 magnets; FT1, FT2, FT3, FT4, FT5 flash-tube trays; GM1, GM2, GM3 Geiger–Müller counter trays. (*a*) Front view; (*b*) side view.

of three Geiger–Müller counter trays for selecting near vertical muons, two solid iron magnets for the deflection of muons, and five flash tube trays for location of their trajectories. A summary of the important features of the spectrograph is given in table 1.

Table 1. Characteristics of the spectrograph

Solid iron magnets
(i) Magnetic volume: $100 \times 75 \times 45$ cm^3 (each magnet)
(ii) Power dissipation: 4·6 kW
(iii) Magnetic induction: $16{\cdot}18 \pm 0{\cdot}14$ kG
(iv) Deflecting power ($\int B\,dl$): $3{\cdot}24 \times 10^6$ G cm
Solid angle of acceptance: 11·6 cm^2 sr
Maximum detectable momentum: 985 ± 25 GeV/*c*
(RMS value)
Ratio of the RMS scattering deflection to the magnetic deflection: 0·17
Total height of the spectrograph: 5·5 m

Each array of flash tubes consists of 120 tubes arranged in eight layers. The flash tubes are 1·55 cm in diameter and approximately 100 cm in length containing neon to a pressure of 60 cm Hg. The horizontal and vertical separation of the tube centres are $1{\cdot}999 \pm 0{\cdot}002$ cm and 2·8 cm respectively.

The variation of the acceptance function of the spectrograph with momentum is shown in figure 2. The acceptance function for particles of a particular momentum is

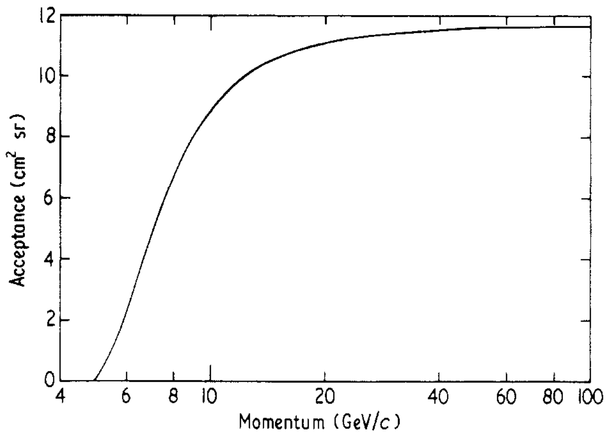

Figure 2. The variation of acceptance function of the spectrograph with momentum.

calculated as follows: a particle of a particular momentum is accepted by the spectrograph if it is incident within a specified range of zenith angles which depend on the position of the particle on the top counter. The maximum and minimum zenith angles in this range, as a function of position on the top counter, are calculated taking into account the energy loss in the magnet blocks. The ratio of the area covered by maximum and minimum zenith angles, within which all particles of a fixed momentum are accepted, to that of a similar area for particles of infinite momentum is calculated. This ratio when multiplied by the geometric acceptance (ie acceptance at infinite momentum) represents the acceptance function for particles of a particular momentum.

The measured spectrum is corrected for the variation of acceptance due to magnetic deflection (as above) and the effect of multiple Coulomb scattering discussed in §4.

3. The collection and analysis of data

The collection of basic data was carried out during the period February 1969 to March 1970. In a running time of 1831 h 25 842 single muons were collected by the spectrograph. As the instrument was symmetric with respect to a vertical line positive and negative particles were accepted with the same probability. The magnetic field was reversed between separate runs in order to remove bias due to variations in the efficiency of the counter system and approximately equal numbers of muons were collected for each field direction.

The trajectories of the particles through five flash-tube trays were recorded photographically. Primarily a track in any one of the five trays was accepted for analysis if at least three tubes flashed with appropriate configuration. If more than one particle passed through any one of the flash-tube arrays, it was accepted if the original triggering particle was identified unambiguously in all the five trays.

The techniques used for the analysis of the flash-tube photographs were the same as described by Hayman and Wolfendale (1962). The maximum detectable momentum was calculated by the method suggested by Allkofer *et al* (1971b) and was found to be 985 ± 25 GeV/c (as shown in the Appendix).

4. Experimental results

An incident comparison spectrum is necessary to compare the experimental muon spectrum with that predicted. The comparison spectrum used here is based on the phenomenological model developed by Barrett *et al* (1952) and Smith and Duller (1959) on the assumption that the π–μ decay process is the only significant source of muons at sea level. Following the treatment of Smith and Duller (1959) the differential intensity of muons at sea level as evaluated by Bull *et al* (1965) is given by

$$F(E_\mu) = \frac{A_\pi P_\mu E_\pi^{-\gamma_\pi} b j_\pi}{E_\pi + b j_\pi}.$$

$A_\pi E_\pi^{-\gamma_\pi}$ is the differential production spectrum of pions, P_μ is the probability of survival to sea level for a muon produced by the decay of pion, $j_\pi = m_\pi x_0 c/\tau_\pi \rho_0$ where m_π, τ_π are the mass and mean life time of pions at rest, x_0 and ρ_0 are the atmospheric depth and density of air corresponding to ground level. The factor $b = 0{\cdot}771$ was introduced by Smith and Duller (1959) in order to correct for the assumption of an isothermal atmosphere.

The momentum spectrum of muons at sea level was determined from the χ^2 test method of comparison of the theoretical deflection spectrum (after correcting for instrumental bias and scattering), with the measured spectrum.

The effect of multiple Coulomb scattering on the spectrum was calculated from the observed deflection distribution by assuming the particles of a particular momentum to have a gaussian distribution of deflection with standard deviation $0{\cdot}17\times$ magnetic deflection and using the method of iteration. The ratio ($=0{\cdot}17$) of the RMS scattering deflection to the magnetic deflection was found to be constant with momentum to within 4%.

The observed momenta were first corrected for the energy loss in the magnet blocks. The deflection spectrum of muons was computed from the above equation for values of γ_π from 2·50 to 2·70 by using Simpson's rule. The predicted number of muons in various deflection categories was corrected for the variation of acceptance function of the spectrograph with momentum (§ 2), the multiple Coulomb scattering in the material of the magnet blocks and the location error of the particle trajectory. To find the number of particles in various deflection categories the theoretical distribution was normalized to the total number of observed particles. For each value of γ_π the degree of correlation between observed and expected deflection spectra was examined by calculating the value of χ^2. The values of χ^2 are plotted as a function of γ_π in figure 3. The best fit value of γ_π corresponding to the minimum value of χ^2 is $\gamma_\pi = 2{\cdot}61^{+0{\cdot}03}_{-0{\cdot}02}$ at the 32% level of significance; the errors correspond to the 16% level of significance.

To determine the constant A_π the total sea-level intensity of muons above 1·0 GeV/c, calculated by integrating the expression, was compared with the absolute integral intensity of muons ($7{\cdot}23\times10^{-3}$ cm^{-2} s^{-1} sr^{-1}) above 1·0 GeV/c measured by Allkofer *et al* (1970b). This procedure gives a value for $A_\pi = 0{\cdot}25$. The spectrum of pions at production can therefore be represented as

$$N(p_\pi)\,dp_\pi = 0{\cdot}25 p_\pi^{-2{\cdot}61}\,dp_\pi.$$

The observed differential intensities given in table 2 and plotted in figure 4 have been calculated by drawing the continuous momentum spectrum with the best-fit value of $\gamma_\pi = 2{\cdot}61$ and plotting the experimental points at the median momentum

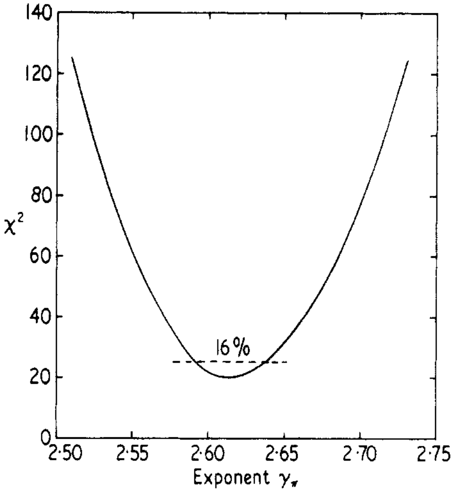

Figure 3. The variation of χ^2 with exponent γ_π for the vertical sea-level muon spectrum.

Table 2. The differential momentum spectrum of muons

Momentum range (GeV/c)	Median momentum (GeV/c)	Number of particles observed	Observed differential intensity (cm^{-2} s^{-1} sr^{-1} (GeV/c)$^{-1}$)	Statistical error (%)
4·85–6·64	5·66	1643	$3{\cdot}83 \times 10^{-4}$	2·5
6·64–7·81	7·20	2627	$2{\cdot}42 \times 10^{-4}$	2·0
7·81–8·94	8·35	2633	$1{\cdot}92 \times 10^{-4}$	2·0
8·94–10·6	9·71	3318	$1{\cdot}40 \times 10^{-4}$	1·7
10·6–13·1	11·8	3989	$9{\cdot}43 \times 10^{-5}$	1·6
13·1–15·1	14·0	2121	$6{\cdot}38 \times 10^{-5}$	2·2
15·1–17·8	16·4	2050	$4{\cdot}21 \times 10^{-5}$	2·2
17·8–21·9	19·7	2064	$2{\cdot}72 \times 10^{-5}$	2·2
21·9–26·9	24·2	1555	$1{\cdot}41 \times 10^{-5}$	2·5
26·9–32·7	29·6	1134	$1{\cdot}01 \times 10^{-5}$	3·0
32·7–42·1	37·1	980	$5{\cdot}40 \times 10^{-6}$	3·2
42·1–52·3	46·9	589	$2{\cdot}99 \times 10^{-6}$	4·2
52·3–69·2	60·0	476	$1{\cdot}45 \times 10^{-6}$	4·6
69·2–103	84·0	367	$5{\cdot}58 \times 10^{-7}$	5·1
103–136	118	131	$2{\cdot}04 \times 10^{-7}$	8·6
136–205	167	84	$6{\cdot}09 \times 10^{-8}$	10
205–339	260	52	$1{\cdot}96 \times 10^{-8}$	13
339–678	467	18	$2{\cdot}69 \times 10^{-9}$	$^{+29}_{-23}$
>678	1109	11	$1{\cdot}03 \times 10^{-10}$	$^{+39}_{-30}$

with an intensity which bears the same relationship to the ordinate of the best-fit spectrum as the observed frequency of events in the deflection cell bears to the expected number. The integral intensities of muons obtained from the present data are given in table 3 and are plotted in figure 5 along with the best-fit integral spectrum. Table 4 gives the differential and integral intensities of muons at various standard momenta.

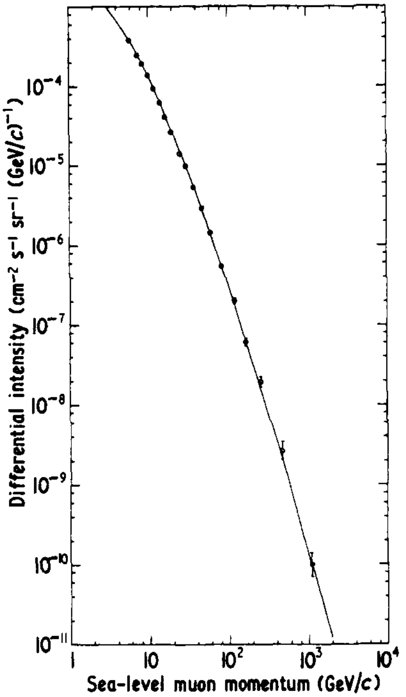

Figure 4. The best-fit differential momentum spectrum of muons together with the experimental points.

Table 3. The integral momentum spectrum of muons

Momentum (GeV/c)	Number of particles observed	Integral intensity ($cm^{-2}\,s^{-1}\,sr^{-1}$)	Statistical error (%)
4·85	25842	$2·28 \times 10^{-3}$	0·6
6·64	24199	$1·60 \times 10^{-3}$	0·6
7·81	21572	$1·31 \times 10^{-3}$	0·7
8·94	18939	$1·09 \times 10^{-3}$	0·7
10·6	15621	$8·62 \times 10^{-4}$	0·8
13·1	11632	$6·27 \times 10^{-4}$	0·9
15·1	9511	$5·13 \times 10^{-4}$	1·0
17·8	7461	$3·88 \times 10^{-4}$	1·2
21·9	5397	$2·90 \times 10^{-4}$	1·4
26·9	3842	$2·05 \times 10^{-4}$	1·6
32·7	2708	$1·43 \times 10^{-4}$	1·9
42·1	1728	$9·10 \times 10^{-5}$	2·4
52·3	1139	$6·03 \times 10^{-5}$	3·0
69·2	663	$3·41 \times 10^{-5}$	3·9
103	296	$1·51 \times 10^{-5}$	5·8
136	165	$8·11 \times 10^{-6}$	7·8
205	81	$3·49 \times 10^{-6}$	12
339	29	$1·12 \times 10^{-6}$	20
678	11	$1·61 \times 10^{-7}$	$^{+39}_{-30}$

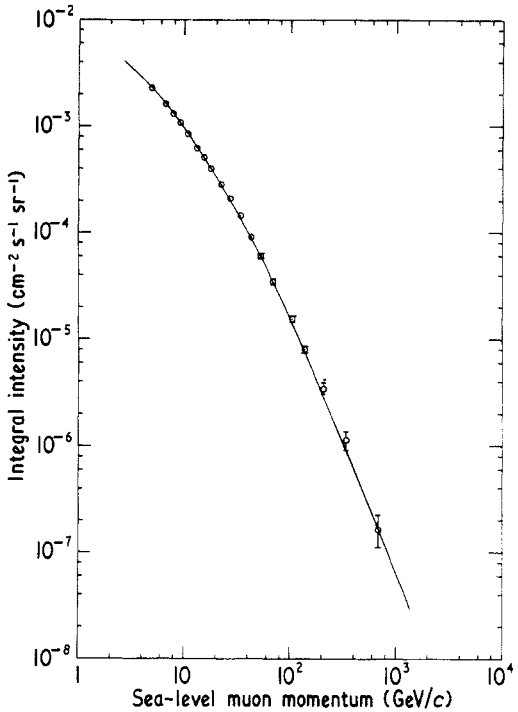

Figure 5. The best-fit integral spectrum of muons together with the experimental points.

Table 4. The differential and integral intensities at standard momenta

Muon momentum at sea level (GeV/c)	Differential intensity ($cm^{-2} s^{-1} sr^{-1} (GeV/c)^{-1}$)	Integral intensity ($cm^{-2} s^{-1} sr^{-1}$)
5	4.70×10^{-4}	2.21×10^{-3}
10	1.30×10^{-4}	9.40×10^{-4}
15	5.39×10^{-5}	5.19×10^{-4}
20	2.73×10^{-5}	3.39×10^{-4}
40	4.55×10^{-6}	9.59×10^{-5}
60	1.46×10^{-6}	4.36×10^{-5}
80	6.24×10^{-7}	2.41×10^{-5}
100	3.18×10^{-7}	1.50×10^{-5}
150	8.97×10^{-8}	5.99×10^{-6}
200	3.56×10^{-8}	3.05×10^{-6}
400	3.53×10^{-9}	5.76×10^{-7}
600	8.75×10^{-10}	2.17×10^{-7}
800	3.25×10^{-10}	1.07×10^{-7}
1000	1.48×10^{-10}	6.16×10^{-8}

6. Comparison with other observations

To determine the shape of the spectrum it has been common practice to normalize to the intensity (2.45×10^{-3} cm^{-2} s^{-1} sr^{-1} $(GeV/c)^{-1}$) given by Rossi (1948) at 1 GeV/c. Recently Allkofer *et al* (1970b) have measured the absolute intensity at 1 GeV/c and found that the intensity is about 25% higher than the Rossi standard intensity. This has been further verified by Ashton *et al* (1971) and Crookes and Rastin (1971).

The intensities obtained by other workers by normalizing at the Rossi point of 1 GeV/c, have been renormalized to the present measurement and compared in figure 6 with the present results. The results of Aurela and Wolfendale (1967), Baber *et al* (1968)

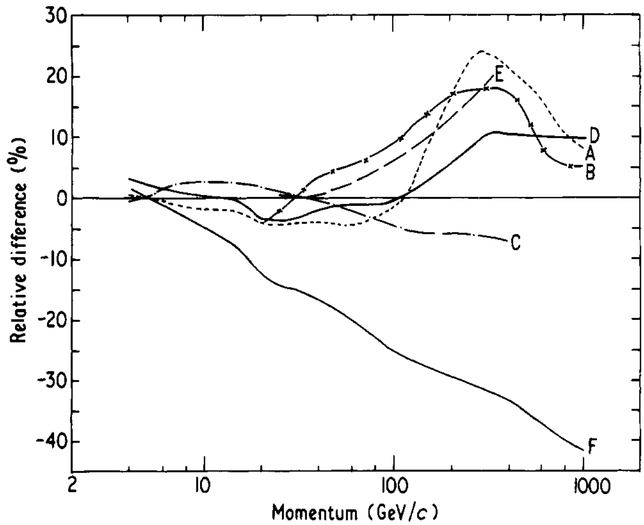

Figure 6. Comparison of the present integral intensity with those obtained by other workers. A Aurela and Wolfendale (1967); B Menon and Ramana Murthy (1967); C Baber *et al* (1968); D Allkofer *et al* (1971a); E Allkofer *et al* (1970a); F Appleton *et al* (1971).

and Appleton *et al* (1971) have been renormalized to the present intensity at 5 GeV/c and the results of Menon and Ramana Murthy (1967) and Allkofer *et al* (1970a) have been renormalized at 20 GeV/c. Within the accuracy of both the measurements the shape of the present spectrum is in good agreement with those of Baber *et al* (1968) and Allkofer *et al* (1971a). The renormalized intensities of Aurela and Wolfendale (1967) are in good agreement with the present results in the momentum range 5–100 GeV/c, but above 100 GeV/c the intensities of Aurela and Wolfendale are higher. The spectrum of Menon and Ramana Murthy (1967) obtained from the survey of various measurements is compared with the present results in curve B. The magnitude of the difference from the present spectrum increases with energy to about 18% higher at 200 GeV/c. The relative difference of the integral intensity of Appleton *et al* (1971) (given by curve F) is negative and its magnitude increases with energy monotonously to 42% at 1000 GeV/c.

It can be concluded that besides the absolute values of the intensities the shapes of the spectrum obtained by various workers are also markedly different.

The spectrum exponent γ_π and the normalization constant A_π obtained by various workers are compared in table 5.

Although the normalization constant ($A_\pi = 0{\cdot}25$) obtained from the present experiment is very close to the value obtained by Baber *et al* (1968) and Appleton *et al* (1971) the higher values of the present intensities are due to a lower value of the exponent ($\gamma_\pi = 2{\cdot}61$).

Table 5. Comparison of A_π, γ_π

Authors	γ_π	A_π
Pine *et al* (1959)	2·64	0·156
Hayman and Wolfendale (1962)	2·67	—
Ashton and Wolfendale (1963)	2·64	0·20
Bull *et al* (1965)	2·67	0·22
Baber *et al* (1968)	2·65	0·24
Appleton *et al* (1971)	2·73	0·24
Present results	2·61	0·25

7. Conclusions

The spectrum has been determined by normalizing the present results to a very recently measured absolute intensity. The main cause of discrepancies between these results and those from other workers is due to the normalization at different absolute intensities.

The present results are consistent with those predicted from the pion diffusion model based on the assumption of pions as the source of muons and a pion production spectrum having a constant exponent. The parameters of the production spectrum determined from the present results are in good agreement with various other measurements. It is not possible to investigate the kaon contribution to the muon beam purely from vertical intensity measurements. From the study of the vertical and inclined muon spectrum Ashton and Wolfendale (1963) and Judge and Nash (1963) have estimated that the K/π ratio is less than 20% for primary energies up to 4×10^{13} eV and 10^{12} eV respectively.

Bergeson *et al* (1967) suggested that the majority of muons observed at sea level above 1000 GeV/c are produced directly or by the decay of very short lived parents (half life $\ll 10^{-8}$ s) instead of by an intermediate stage involving pions or kaons. In view of this interpretation, precise measurements of the momentum spectrum of muons at momenta higher than that discussed here are of great importance not only in the vertical direction but also at large zenith angles. Such measurements are in progress in a number of laboratories.

Acknowledgments

The authors wish to express their sincere thanks to Professor A W Wolfendale of the University of Durham, UK for his keen interest and valuable advice during the progress of this work and the University of Durham for generous help. The financial assistance from the Department of Atomic Energy, Government of India for sponsoring this project is gratefully acknowledged.

Appendix. Maximum detectable momentum of the spectrograph

A general formula for maximum detectable momentum (MDM) of a spectrograph has recently been derived by Allkofer *et al* (1971b) assuming that (i) the spectrograph consists of a uniform magnetic field region of length h in which the effective magnetic induction is Bl/h, where l is the total length of all magnets, (ii) the detectors are placed symmetrically with respect to the x axis (figure 7), (iii) the projected trajectory of the particle in

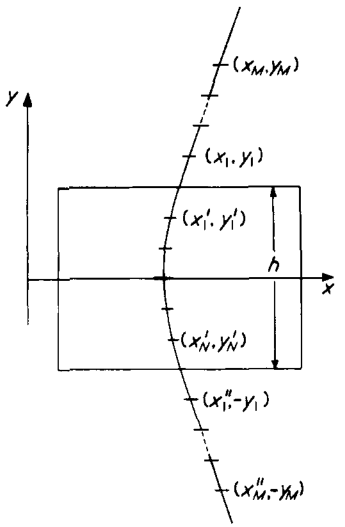

Figure 7. Coordinate system used for calculation of MDM.

the magnetic field is approximated by a parabola. From the best fit condition the following general formula for MDM has been derived:

$$p_{\text{MDM}} = \frac{150Bl}{h\sigma_x} S^{1/2}$$

where σ_x is the RMS error in the location of trajectory and

$$S = \sum_{i=1}^{N} y_i'^4 + h^2 \sum_{k=1}^{M} (2y_k^2 - hy_k) + \frac{Mh^4}{8} - \frac{(\Sigma_{i=1}^{N} y_i'^2 + 2h\Sigma_{k=1}^{M} y_k - \frac{1}{2}Mh^2)^2}{N+2M}$$

where N is the number of detectors within the magnet region and $2M$ is the number of detectors outside this region. In the present case $N = 1$, $2M = 4$ and hence $S = 1{\cdot}69 \times 10^9\ \text{cm}^4$. For $\sigma_x = 0{\cdot}75$ mm, the MDM of the spectrograph is 985 ± 25 GeV/c.

References

Allkofer O C, Cartensen K and Dau W D 1971a *Proc. 12th Int. Conf. on Cosmic Rays, Hobart* vol 4 (Hobart: University of Tasmania) pp 1314–8

Allkofer O C *et al* 1970a *Acta. Phys. Hung.* **29** *Suppl.* 4 13–8

Allkofer O C, Carstensen K, Dau W D and Jokisch H 1971b *Proc. 12th Int. Conf. on Cosmic Rays, Hobart* vol 4 (Hobart: University of Tasmania) pp 1596–601

Allkofer O C, Dau W D and Jokisch H 1970b *Proc. 6th Interamerican Seminar on Cosmic Rays La Paz, Bolivia*

Appleton I C, Hogue M T and Rastin B C 1971 *Nucl. Phys.* B **26** 365–89

Ashton F, Tsuji K and Wolfendale A W 1971 to be published

Ashton F and Wolfendale A W 1963 *Proc. Phys. Soc.* **81** 593–603

Aurela A M and Wolfendale A W 1967 *Ann. Acad. Sci. Fenn.* AVI **227** 1–14

Baber S R, Nash W F and Rastin B C 1968 *Nucl. Phys.* B **4** 539–49

Barrett P H *et al* 1952 *Rev. mod. Phys.* **24** 133–78

Bergeson H E *et al* 1968 *Phys. Rev. Lett.* **21** 1089–93
Bull R M, Nash W F and Rastin B C 1965 *Nuovo Cim.* **40** 365–84
Crookes J N and Rastin B C 1971 *Proc. 12th Int. Conf. on Cosmic Rays, Hobart* vol 4 (Hobart: University of Tasmania) pp 1325–8
Hayman P J and Wolfendale A W 1962 *Proc. Phys. Soc.* **80** 710–28
Judge R J R and Nash W F 1963 *Proc. Int. Conf. on Cosmic Rays, Jaipur* vol 6 (Bombay: Department of Atomic Energy) pp 60–3
Menon M G K and Ramana Murthy P V 1967 *Prog. elem. Part. cosm. Ray Phys.* **9** 161–243
Nandi B C and Sinha M S 1970 *Acta. Phys. Hung.* **29** *Suppl.* 4 529–33
Pine J, Davisson R J and Greisen K 1959 *Nuovo Cim.* **14** 1181–203
Rossi B 1948 *Rev. mod. Phys.* **20** 537–83
Smith J A and Duller N M 1959 *J. Geophys. Res.* **64** 2297–305